Synthesis and Characterization of Santa Barbara Amorphous (SBA-15) for CO_2/CH_4 Separation

by

Chua Yin Ching

14771

Dissertation submitted in partial fulfilment of
the requirements for the
Bachelor of Engineering (Hons)
(Chemical)

JANUARY 2015

Universiti Teknologi PETRONAS
Bandar Seri Iskandar
31750 Tronoh
Perak Darul Ridzuan

CERTIFICATION OF APPROVAL

Synthesis and Characterization of Santa Barbara Amorphous (SBA-15) for CO_2/CH_4 Separation

by

Chua Yin Ching

14771

A project dissertation submitted to the
Chemical Engineering Programme
Universiti Teknologi PETRONAS
in partial fulfilment of the requirement for the
BACHELOR OF ENGINEERING (Hons)
(CHEMICAL)

Approved by,

____

(Dr. Oh Pei Ching)

UNIVERSITI TEKNOLOGI PETRONAS
TRONOH, PERAK
January 2015

CERTIFICATION OF ORIGINALITY

This is to certify that I am responsible for the work submitted in this project, that the original work is my own except as specified in the references and acknowledgements, and that the original work contained herein have not been undertaken or done by unspecified sources or persons.

CHUA YIN CHING

ABSTRACT

This project main focus is to identify the potential inorganic filler to be used for mixed matrix membrane (MMM) fabrication. The properties of polymeric membrane have been well understood as it is widely implemented in current industry. The identified inorganic filler is Santa Barbara Amorphous (SBA-15) mesoporous silica. It will be synthesized in nano-scale to answer the problem of particle agglomeration faced by current membrane research. Having considerably high CO_2 permeability and CO_2/CH_4 selectivity, SBA-15 is then being functionalized with amino-propyl group by incorporating APTES onto the surface of the silica to further enhance its performance. Polysulfone (PSf) is chosen to be the polymer for this project. MMM of PSf/pristine SBA-15 and PSF/modified SBA-15 are fabricated and characterized to observe its morphology in supporting gas separation performance. TGA result shows almost all membranes share the similar onset decomposition temperature at around 500°C. FESEM analysis shows there are minimal interfacial voids formed between SBA-15 fillers and PSf polymer chain, which indicates that there is good adhesion between the filler and polymer chosen. Although the distribution of SBA-15 filler get better when its loading increases, particles agglomeration is observed to be increasing as well. Hence, SBA-15 with 3wt% loading is concluded to be the optimum percentage to be incorporated into MMM. From the result interpretation, it is believed that MMMs with incorporation of either pristine or functionalized SBA-15 fillers are expected to enhance its gas separation performance, as comparison to that of PSf membrane.

ACKNOWLEDGEMENT

I would like to express my deepest appreciation to all those who provided me the possibility to complete this report. A special gratitude I give to my final year project supervisor, Dr. Oh Pei Ching, whose contribution in stimulating suggestions and encouragement, helped me to coordinate and complete my project within the given time frame. She has been very helpful in guiding and advising me to improve on this project quality, not to forget the financial support that she has given me through her research grant in completing this project. I am truly blessed in getting an understanding and helpful project supervisor who gives constant guidance and supervision as well as providing necessary directions in completing this project.

My thanks and appreciations also go to my beloved parents and for their endless encouragement which managed to help me pull through until the end. My gratitude also goes to UTP staffs especially the technicians in Block 3, 4 and 5 for their assistance and co-operation. Not forgetting to thank FYP coordinator, Dr Asna, in arranging the evaluation sessions for us. Lastly, I would like to express my gratitude to towards my friends in showing their love and support whenever I need them.

I have put on efforts to this project, but it would not have been possible without the kind support and help of above mentioned individuals and organization.

TABLE OF CONTENT

LIST OF FIGURES

LIST OF TABLES

CHAPTER 1

INTRODUCTION

1.1 BACKGROUND

1.1.1 Carbon dioxide, CO_2 Separation from Natural Gas, CH_4

CO_2 is the largest contaminant found in natural gas and the major contributor for the global greenhouse gases (GHG) emissions. The high content of CO_2 in natural gas which is around 80% of it must be strictly reduced for a number of reasons. The acidity of CO_2 actually corrodes the equipment and pipelines transporting these gases. So by reducing the content of acid gas, we can reduce the size of this equipment and in line with it, increasing the heating value as well. Heating value or calorific value is the heat released from combusting a unit of natural gas (Rezakazemi, Ebadi Amooghin, Montazer-Rahmati, Ismail, & Matsuura, 2014). By removing CO_2 from natural gas, we are supplying effective and efficient fuel to be used in energy generation. In addition, CO_2 is an economic source in enhanced oil recovery (EOR). The property of CO_2 which is miscible with oil makes it possible to increase the mobility of oil under the rocks.

1.1.2 Gas Separation Technology

Since it is a dire need to separate CO_2 from natural gas, there has been many gas separation technology been developed and discovered. It can be divided into four main techniques which the industries usually used, which are Swing Adsorption Techniques, absorption, cryogenic distillation and membrane gas separation. The details of these techniques are summarized into Figure 1.1 below**:**

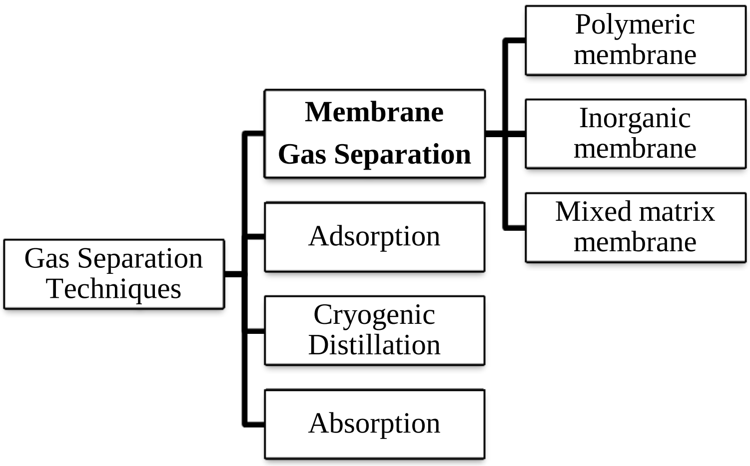

Figure 1.1: Three types of gas separation techniques

Swing adsorption techniques such as pressure and temperature swing adsorption are the few techniques that are commercially used in the industries to remove CO_2 from natural gas and for hydrogen, H_2 production as well. This adsorption technology is not quite an attractive choice to separate CO_2 from flue gas because CO_2 selectivity of available adsorbents is low. However, it can be a successful achievement in the future if it combines with other capture technology.

Gas separation membranes allow one component in a gas stream to pass through faster than the others. This technique usually does not have high degrees of separation, so a recycle stream or multiple stages are needed in membrane separation technology. In cryogenic distillation, CO_2 is separated by cooling and condensing, and is used when there is high concentration of CO_2 only.

1.1.3 Polymeric Membrane

Polymeric membranes have been used in a wide range of industrial applications such as CO_2/N_2 and CO_2/CH_4 gas separation processes. These membranes have some remarkable advantages such as low energy requirements, easy of fabrication and good thermal and mechanical resistance (Moghadassi, Rajabi, Hosseini, & Mohammadi, 2014). Despite these advantages of polymeric membranes, polymeric membranes are limited by the upper bound Robeson trade-off curve.

For any of particular gas pair, the fundamental parameters characterizing membrane separation performance are permeability coefficient, P_A and selectivity,

$\alpha_{A/B}$. The permeability coefficient is the product of gas flux and membrane thickness divided by the pressure difference across the membrane. Gas selectivity is the ratio of permeability coefficients of two gases ($\alpha_{A/B} = P_A/P_B$), where P_A is the permeability of the more permeable gas (CO_2) and P_B is the permeability of the less permeable gas (CH_4) in the binary gas pair. A general trade-off relation has been recognized between permeability and selectivity. Polymers which give high permeability values has lower selectivity values (Freeman, 1999; Staiger, Pas, Hill, & Cornelius, 2008).

A feature of high selectivity and high selectivity is a must in synthesizing an ideal gas separation membrane. Even after extensive studies have been done for the gas permeation properties, there are still strong trade-off relations of gas permeability and selectivity in polymeric membranes that will not be easily broken in the future. Based on numerous references, Robeson had finally come out with the trade-off relations of polymeric membranes with various gas pairs (Li, Fane, Ho, & Matsuura, 2011; Moghadassi et al., 2014).

In this project, the gas pair that we are investigating is CO_2/CH_4. Figure 1.2 shows the upper bound line of CO_2 permeability and CO_2/CH_4 perm selectivity. The doted red and straight blue lines represent the best combination of selectivity and permeability values, which respectively was discovered in 1991 and 2008.

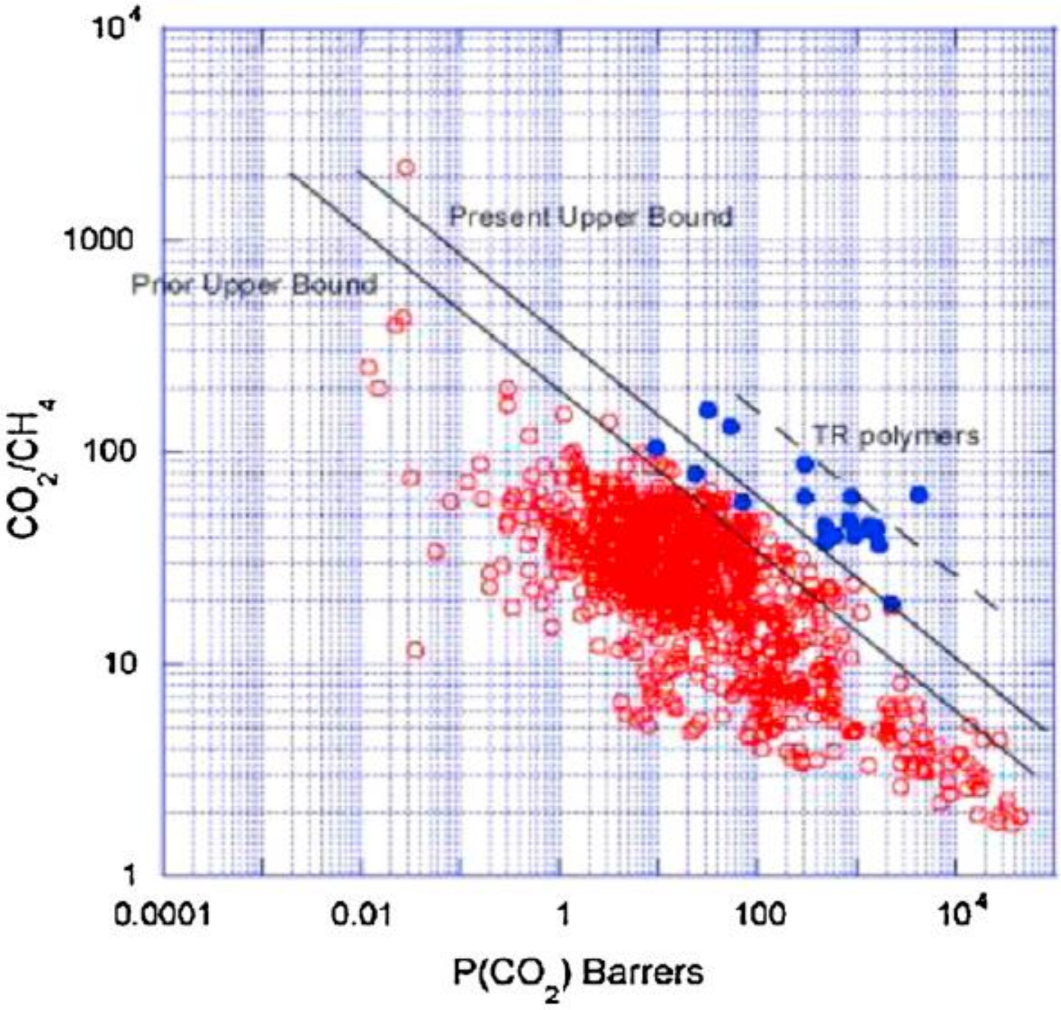

Figure 1.2: Robeson trade-off curve for CO_2/CH_4 selective polymeric membranes.

1.1.4 Inorganic Membrane

Inorganic membranes refer to membranes made of materials such as ceramic, carbon, silica, zeolite, various oxides and metals such as palladium, silver and their alloys. It can be categorized into two main elements, such as porous inorganic membranes and non-porous or dense inorganic membranes.

Inorganic membranes are potentially useful in gas separation technology and have been applied in the industrial scale in recent years. If the feed or product gases can be separated at elevated temperatures specific to each process, the energy required for purification could be greatly reduced (Morooka & Kusakabe, 1999). The permeation rate and perm selectivity of porous inorganic membranes are heavily dependent on the structure of the membrane such as pore size and distribution, porosity and the affinity between permeating species and pore walls. However, inorganic membrane has a major drawback, which is having extremely high sensitivity to temperature gradient. This problem has led to membrane cracking due to the brittleness affected by high temperature. This inorganic membrane application also faces difficulty in proper sealing of the membrane operating at high temperature.

1.1.5 Mixed Matrix Membrane (MMM)

Mixed matrix membranes (MMM) are a well-known route to enhance the properties of polymeric membranes. Their microstructure consists of an inorganic material in the form of micro- or nano-particles incorporated into a polymeric matrix. The use of two materials with different flux and selectivity provides the possibility to better design a membrane for CO_2 capture, allowing the superior gas separation performance of inorganic materials. Furthermore the addition of inorganic materials in a polymer matrix offers enhanced physical, thermal and mechanical properties for aggressive environments and represents a way to stabilize the polymer membrane against change in perm-selectivity with temperature (Brunetti, Scura, Barbieri, & Drioli, 2010; Hu et al., 1997).

Figure 3 below shows an example of MMM formation mechanism. The advantages from both polymeric and inorganic are combined and the disadvantages are somehow minimized to get a better gas separation performance of MMM. Water or gas molecules can diffuse at the interface between the polymer matrix and the nano-particles to give a membrane with enhanced flow properties (He et al., 2011).

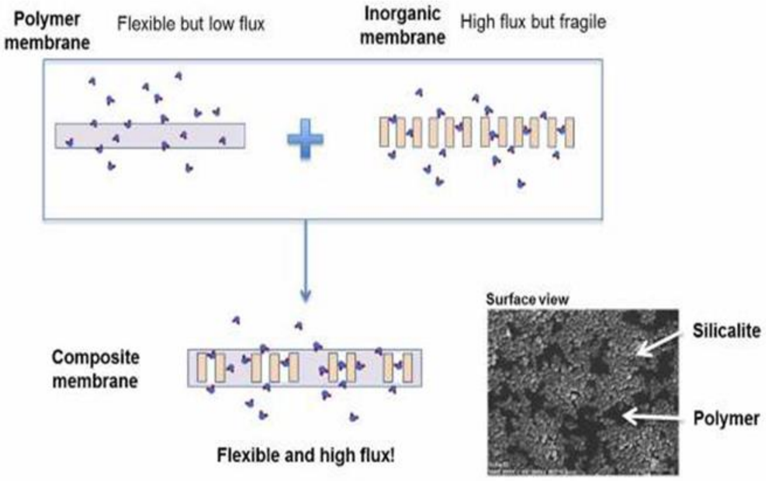

Figure 1.3: Synthesizing a mixed matrix membrane using polymer/nano-particle solvent casting (He et al., 2011).

Table 1 below shows the comparison of three types of membrane separation techniques, at which the plus points are all gathered under the column of MMM.

Table 1.1: Comparison of different types of membrane separation techniques (Luan, Fournier, Wooten, & Miser, 2005)

	Polymeric membrane	***Inorganic membrane***	***Mixed matrix membrane***
Cost	Cheap	Expensive	Moderate
Thermal stability	Unstable Temperature limited	Some have low hydrothermal stability	Better thermal stability
Permeability	Usually high	Usually low	Improved permeability
Selectivity	Usually low	Usually high	Improved selectivity
Structure	Weak Prone to denature	Brittle	Better structure, more rigid

1.2 PROBLEM STATEMENT

Carbon dioxide, CO_2 or acid gases must be removed from natural gas before consuming to avoid the corrosion of equipment and pipelines. Membrane gas separation technology is one of the solutions to it. The concept of mixed matrix membrane (MMM), a combination of polymer matrix and inorganic materials, has been the focus of future applications. A reliable and industrially qualified MMM for CO_2/CH_4 gas separation demands a full understanding of separation mechanism in the membrane material. Nevertheless, as the properties of polymer matrix in separation have been well understood in proven technologies, the rate of progress in understanding of inorganic materials is still far well behind. This has then created the limitations in finding the optimum membrane dope formulation to synthesize a competitive MMM in industrial scale. The concern of both permeability and selectivity of the possible combination of polymer matrix and inorganic materials is another challenge in fabricating MMM with excellent gas separation performance.

1.3 OBJECTIVES

- To synthesize Santa Barbara Amorphous (SBA-15) mesoporous silica.
- To functionalize the synthesized SBA-15 mesoporous silica with (3-aminopropyl) triethoxysilane (APTES).
- To characterize the pristine and functionalized SBA-15 mesoporous silica using Transmission Electron Microscope (TEM), Fourier Transform Infra-Red (FTIR) and Surface Area Analyzer and Porosimetry System (SAP).
- To elucidate the casting solution formulation for synthesis of pristine polysulfone (PSf) membrane and mixed matrix membrane (MMM).
- To characterize the resultant membranes using Thermal Gravimetric Analyzer (TGA) and Field Emission Scanning Electron Microscope (FESEM).

1.4 SCOPE OF STUDY

SBA-15 mesoporous silica, which exhibits a remarkable hydrothermal stability, is the choice of inorganic material in this study. It will be synthesized in the lab in the very beginning to be used in the fabrication of MMM in the later step. Pluronic 123 is a chemical which acts as a templating surfactant in the synthesis of pristine SBA-15 will be used. After SBA-15 mesoporous silica powder is obtained, functionalization will be performed. The purpose of this step is to investigate the performance of modified SBA-15 in gas separation field. In this study, aminopropyl groups are used and APTES is added to modify SBA-15 mesoporous silica.

Characterization of both SBA-15 and modified SBA-15 must be performed to analyze the surface area and pore capacity for adsorption. The surface and cross-section morphology of the samples will be observed and analyzed from TEM, while FTIR spectra of functionalized SBA-15 will decide whether or not functionalization is successful. The nitrogen adsorption or desorption isotherms can be obtained and analyzed from Porosimetry System.

There are quite a number of methods for membrane fabrication in details. Some examples are phase inversion method and casting solution method. In this study, we need to fabricate three membranes: PSf polymeric membrane, pristine SBA-15 MMM and also modified SBA-15 MMM. The weight percent of polymer and solvent are the two manipulated variable that need to be focused on to obtain a good piece of membrane for analysis and testing purpose. The resultant membranes will then be characterized by using analytical tools such as FESEM and TGA to predict the gas separation performance.

CHAPTER 2

LITERATURE REVIEW AND / OR THEORY

2.1 Introduction to SBA-15 Mesoporous Silica

Inorganic materials are the components that will be combined with polymer matrix for MMM fabrication. Some examples of inorganic materials consist of zeolite, newly discovered carbon nano-tubes, carbon molecular sieve and silica nano-particles. The successful implementation of MMM depends greatly on the polymer matrix selection, the inorganic filler and also the interaction between these two phases. Among the mentioned inorganic materials, silica nano-particles gathered the most attention of researchers because of its adsorption capabilities and porous structure. Mesoporous silica, such as MCM-41 and SBA-15, are solid materials which are comprised of a honeycomb-like porous structure with hundreds of empty channels or mesopores that are able to adsorb relatively large amount of molecules. The unique properties such as high surface area, large pore volume and tunable pore size with a narrow distribution, of these materials make them potentially suitable for gas separation applications (Vivero-Escoto, Slowing, Trewyn, & Lin, 2010).

SBA-15 is mesoporous silica which has cylindrical pores arranged in a hexagonal order synthesized with Pluronic triblock-copolymer P123. The structure of SBA-15 is shown in Figure 2.1 below. For this material, the pore size refers to the width of the cylindrical pores which can be tuned between 4-26 nm (Cao, Man, & Kruk, 2009; Johansson, 2010; Zhao, Huo, Feng, Chmelka, & Stucky, 1998) even though the pore sizes above 12nm are rare.

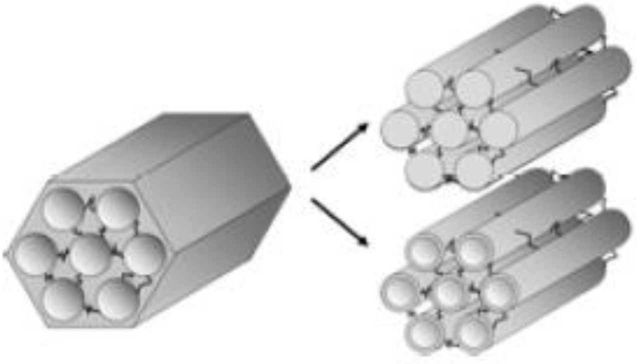

Figure 2.1: The structure of mesoporous silica SBA-15 (to the left) and its replica in form of rods (top right) and straws (down right) (Johansson, 2010).

2.2 SBA-15 Synthesis

The formation mechanism of SBA-15 is assumed to be similar to the formation of MCM-41 which was suggested by Beck *et al*. to be a liquid crystal mechanism (Beck et al., 1992). This can be seen in Figure 2.2 below and shows how the micelles starts as spherical and when the silica precursor is added, the micelles becomes elongated and arranges themselves in a hexagonal pattern while the silica walls are built. After calcination, the surfactants are removed and only the mesoporous silica remains.

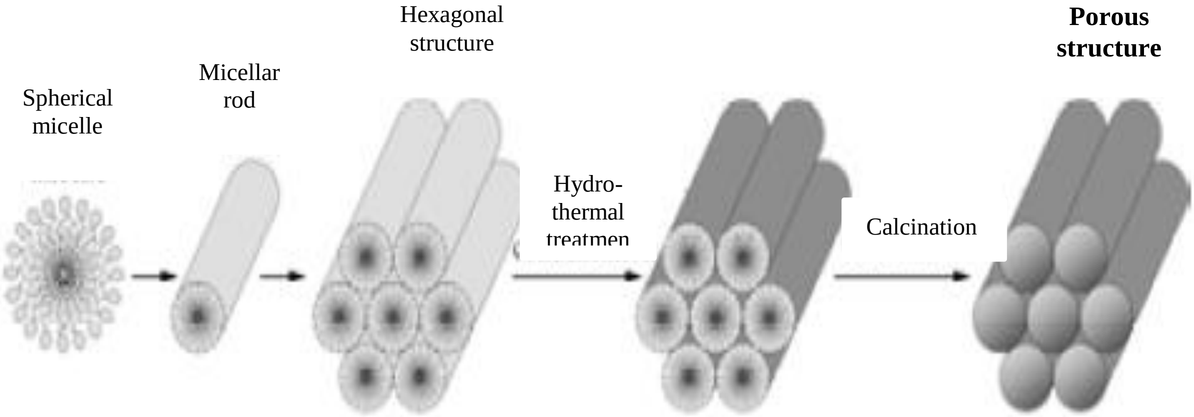

Figure 2.2: Illustration of the formation mechanism of SBA-15 (Beck et al., 1992).

During hydrothermal treatment of SBA-15, Pluronic 123 which is temperature dependent, will play a role in tuning the pore size, micropore volume and the surface area of the final product. By increasing the hydrothermal treatment temperature from 35-130°C, the tendency of increasing the mesopore sizes increases (Beck et al., 1992).

The purpose of calcination is to remove the surfactant from the final product. Beck et al. also reported that the material is heated in air to 550°C for continuously 5 hours. It is then cooled down to the room temperature (Beck et al., 1992). Nevertheless, some past studies suggested the calcination period to be 4 hours at 139°C (Kruk, Jaroniec, Ko, & Ryoo, 2000), 6 hours at 549°C (Srivastava, Srinivas, & Ratnasamy, 2005) and 6 hours at 539°C (Yan, Komarneni, & Yan, 2013). Besides, calcination surfactant also can be removed by solvent extraction in order to preserve the integrity of organic species (Iglesias, Melero, & Sainz-Pardo, 2008).

2.3 Functionalization of SBA-15

Modified mesoporous materials are prepared by functionalizing the surface of the materials with organic groups. Organically functionalized mesoporous materials have generated a great deal of interest in their application in the field of catalysis, sensing, and adsorption due to their high surface areas and large ordered pores ranging from 20 to 300 Å1-5 with narrow size distributions (Margolese, Melero, Christiansen, Chmelka, & Stucky, 2000).

Further functionalization of mesoporous materials was usually done to improve its chemical and physical properties, as well as another alternative in improving the adsorption capability during membrane fabrication process.

There are two major ways to functionalize the surface of mesoporous silicates by organic functional groups, named as post-synthesis grafting and co-condensation. Each of these two functionalization methods has certain advantages and is tabulated below (Huang, 2009):

Table 2.2: Two methods of functionalization

Post-synthesis Grafting Method	**Co-condensation Method**
• To modify a pre-fabricated inorganic mesoporous material surface by attachment of functional groups to the surface of material, usually after surfactant removal. • The original structure of the mesoporous support is generally maintained after grafting. • The external surface is more accessible and is functionalized predominantly over the internal mesopore surface.	• Another strategy to functionalize mesoporous silicates' surface by sol-gel chemistry between tetraalkoxysilane and one or more organoalkoxysilanes with Si-C bonds. • Able to give homogeneously distributed organic groups on the entire inner pore surfaces and no pore-blockage or shrinkage problems. • Provides a uniform surface coverage.

2.3.1 Selection of Amine Group for Modification of SBA-15

The incorporation of organic amines into a porous support is a promising approach for CO_2 sorbents combining good capacity and selectivity at moderate temperature. Amine functional groups are useful for CO_2 removal because of their ability to form ammonium carbamates and carbonates reversibly (Zheng et al., 2005). Various porous supports with the impregnation of liquid amines had been given problems such as loss due to evaporation at a moderate temperature. By grafting of amine functional groups directly to the surface of a physical sorbent, the evaporation problem is eliminated and the overall thermal stability can be improved (Zheng et al., 2005). So, further study has been done of impregnating liquid amine instead of solid one for better performance.

According to Sakpal et al., the silica surface is quite complex and contain more than one type of hydroxyl groups. Out of the three types of hydroxyl groups, the first one is a single hydroxyl group attached to a silicon atom which has three siloxane bonds connecting it to the gel matrix. The second one is two hydroxyl groups attached to the same silicon atom, which in turn is connected to the matrix by two siloxane bonds. These twin hydroxyl groups are called germinal hydroxyl groups. The third one has three hydroxyl groups attached to a silicon atom, which in turn is connected to the silica matrix by only a single siloxane bond. As shown in Figure 6 below, the interaction between the amine functionalized silica surface and CO_2 molecules is thought to result in the formation of ammonium carbamates under anhydrous conditions and ammonium bicarbonate and carbonate species in the presence of water (Sakpal, Kumar, Kamble, & Kumar, 2012).

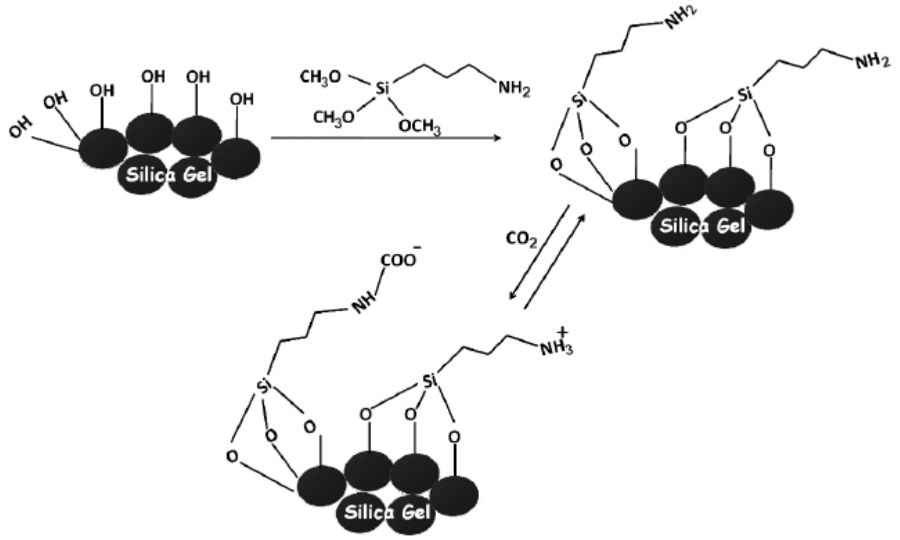

Figure 2.3: Mechanism of reaction of CO_2 with amine loaded silica surface (Sakpal et al., 2012)

2.3.1.1 Functionalization of SBA-15 with 3-aminopropyl triethoxysilane (APTES) from Amine Group

APTES were previously incorporated into zeolites, which contain regular arrays of uniformly sized channels of less than 15 Å. However, the attempts of doing so have met with little success because APTES could not be found in the micropores of zeolite after the impregnation (Luan et al., 2005). This probably was because of the minute micropore sizes of zeolite which is less than 2 nm. Hence, the study of modifying SBA-15 with APTES came out since SBA-15 has better thermal and hydrothermal stability.

The XRD patterns of the APTES-modified SBA-15 do not show any significant difference from the parent SBA-15. This proves that the inorganic wall structure of the SBA-15 silica still remains intact after the modification process. Finally, Luan *et al*. concluded that the incorporation process is highly convenient and effective in terms of controlling the molar loading up to about 13% with respect to silicon (Luan et al., 2005).

However, there are a few challenges need to be faced while carrying out the experiment. Amine group of APTES is easily protonated under acidic solution, such protonated amine group would have cross-linked with silanol groups of the silicate species resulting in disruption of silica walls (Luan et al., 2005; Maria Chong & Zhao, 2003). Precautions have to be taken when running the experiment to avoid APTES being easily protonated. Another challenge is that the balancing of APTES: TEOS molar ration. Maria Chong et al. reported that samples synthesized with APTES: TEOS $\leq$ 15 possess a much better order than samples synthesized with APTES: TEOS $\geq$ 10. This indicates that there is an optimum range of molar ratio of APTES: TEOS that can be employed to synthesize functionalized SBA-15 with a high loading of functionality yet a good mesostructure (Maria Chong & Zhao, 2003).

2.4 Selection of Polymer for Polymeric Membrane and MMM Fabrication

The application of polymeric membrane in gas separation industries is very well developed as they are cheaper compared to inorganic membrane. They do have excellent mechanical stability under high pressure, not forgetting the east of its fabrication. However, the main problem with polymeric membrane is that the unbalance of permeability and selectivity values. A number of studies had been done and it is proven that there is an inverse relationship between permeability and selectivity (Freeman, 1999; Li et al., 2011; Rezakazemi et al., 2014; Zhang, Sunarso, Liu, & Wang, 2013). In searching for a suitable polymer, it is needless to mention that the balancing of these two values is essential to take note of. Robeson’s upper bound trade-off curve, which has been discussed in the early part, is considered the benchmark in gas permeation membrane separation (Zhang et al., 2013).

Zhang et al also reported that the issue of plasticization is of particular concern for CO_2/CH_4 separation as well, especially when there is high content CO_2 in the stream. CO_2-induced plasticization refers to a phenomenon where the CO_2 permeability increases as a function of pressure while the selectivity deteriorates (A. Ismail & Lorna, 2002).

2.4.1 Fabrication of polysulfone (PSf) Polymeric Membrane

Polysulfone (PSf) is the chosen polymer and N-Methyl-2-pyrrolidone (NMP) and double-distilled water (DDW) were used as the solvent and the non-solvent, respectively in this part of membrane fabrication. Composite membranes were prepared by the phase inversion method (Eren, Sarihan, Eren, Gumus, & Kocak, 2015).

2.4.2 PSf as a Chosen Polymer

After further analysis of few potential polymers, PSf is chosen because of its higher permeability and selectivity values override the others. Having a permeability of 80.7 Barrer and CO_2/CH_4 selectivity of 40.2, PSf is a thermoplastic polymer with excellent toughness and stability under high temperature. PSf is one of the most widely investigated glassy polymer membrane materials for CO_2/CH_4 separation. PSf pure- and mixed-gas permeation properties have been extensively explored for gas separation due to its low price, chemical stability, and mechanical strength (Julian & Wenten, 2012). In terms of CO_2 permeability and CO_2/CH_4 selectivity, cellulose acetate (CA) shows better performance as compared to PSf. Nevertheless, PSf has higher plasticization pressure than CA. Membrane with higher plasticization pressure can maintain its selectivity better than membrane with lower plasticization pressure on high CO_2 feed concentration or on high operation pressure (Julian & Wenten, 2012). Table 3 below shows some significant figures of PSf which make it stands out to be chosen for membrane fabrication.

Table 2.2: Characteristics of PSf polymer (A. F. Ismail & Mansourizadeh, 2010)

Feature	Value
CO_2 permeability	80.7 GPU
CO_2/CH_4 selectivity	40.2
Plasticization pressure	30 bar

2.5 Concept of Mixed Matrix Membrane (MMM)

Many MMM related research papers are working on finding the best combination of porous inorganic materials with polymer matrices where it can boost up the gas separation technology in current industries. The two materials are required to be selective for the same gas pairs, and in most case, the inorganic fillers may have the selectivity far superior to the neat polymer (Chung, Jiang, Li, & Kulprathipanja, 2007). Hence, the incorporation of a very small amount of inorganic fillers into the polymer matrix can result in obvious increase in overall separation efficiency.

Even though the selection of appropriate inorganic filler was the major concern in the early development of MMMs, it has been found that the choice of a suitable polymer as the matrix is also important in determining the MMM performance (Chung et al., 2007). Therefore Chung *et al*. concluded that, the suitable combination of polymer and inorganic filler is critical for MMM development. The ratio of the resistance presented to the gas transport by the two phases will determine the minimum membrane performance in the absence of defects.

CHAPTER 3

METHODOLOGY / PROJECT WORK

3.1 Experimental Procedure: Synthesis of Pristine SBA-15

1) 2.0 g of Pluronic 123 (gel form) is dispersed in 15.0 mL distilled water. This mixture is stirred continuously with at temperature of 40°C.
2) After Pluronic 123 gel is fully dissolved, 40.3 mL of 2 M HCl (calculation shown in Appendix) is added while stirring.
3) 4.5 mL of TEOS is added next. The solution is continuously stirred until it is homogenous.
4) The solution is then left to be stirred for 24 hours at 40°C.
5) The cloudy mixture is then aged in a Teflon bottle under hydrothermal conditions at 100°C for 48 hours.
6) After cooling down Teflon bottle to room temperature, the mixture is filtered and the residue is the desired SBA-15 mesoporous silica. Teflon bottle is rinsed with deionized water.
7) The filtrate in the Erlenmeyer flask is kept and labelled.
8) Upon transferring it to another Erlenmeyer flask, the desired product is then washed with deionized water for three times.
9) The filtrate in the second flask is also kept and labelled separately.
10) The product on the filter paper is then opened up and dried in open air for at least 48 hours.
11) Once the weight of product is constant, it is calcined in furnace at 550°C for 24 hours.
12) The final solid product is then weighed to obtain the product yield.

3.2 Experimental Procedure: Synthesis of Functionalized SBA-15

1) 1.0 g of dried SBA-15 powder is added to 10 mL of dry toluene solution containing 1.0g of APTES.
2) Solution is stirred at room temperature until SBA-15 is fully dissolved.
3) The cloudy mixture is then aged in a Teflon bottle under hydrothermal conditions at 100°C for 24 hours.
4) After cooling down Teflon bottle to room temperature, mixture is filtered and the residue is the desired APTES-modified SBA-15 mesoporous silica. Teflon bottle is rinsed with dry toluene.
5) The filtrate in the Erlenmeyer flask is kept and labelled.
6) Upon transferring it to another Erlenmeyer flask, the desired product is then washed with dry toluene followed twice by dichloromethane (DCM).
7) The filtrate in the second flask is also kept and labelled separately.
8) The product on the filter paper is then and dried at 120°C for 12 hours.
9) The final solid product is then weighed again to obtain the product yield.

3.3 Experimental Procedure: Fabrication of Polysulfone (PSf) Membrane

1) PSf pallets are dried in drying oven at 60-80 ºC for 24 hours to remove moisture.
2) 25 wt% of PSf and 75 wt% of NMP solvent are used (calculations shown in Appendix).
3) 7.83 mL of NMP solvent is stirred on a hot plate at a temperature of 50 ºC.
4) 2.69 g of dried PSf pallets is slowly added into NMP while stirring.
5) Until all PSf is added, heating is stopped while mixture is continuously left to stir for 12 hours.
6) Dope solution is then transferred to a centrifugal tube and sealed with parafilm for degassing purpose.
7) Degassing is carried out for 4 hours to remove the gas bubbles in dope solution.
8) After degassing is done, dope solution is left for standing in the lab at room temperature for 24 hours.
9) Dope solution is again put for degassing for 30 minutes and leave for standing 30 minutes to fully remove additional gas bubbles if necessary.
10) A clean glass plate is washed with acetone and dried completely using compressed air.
11) Dope solution is now ready to be casted. The homogenous mixture is poured onto the glass plate.
12) Membrane casting is then performed with the casting knife and film thickness is 200 µm.
13) The casting knife is pulled from upper to lower of the glass plate to form the membrane film. Speed should be consistent to prevent defects.
14) After casting, film is left to evaporate for 10 minutes on the glass plate.
15) Then, glass pate is immersed into coagulation bath which is half filled up with distilled water for 24 hours.
16) Membrane is finally dried at room temperature for another 48 hours.

3.4 Experimental procedure: Fabrication of PSf/SBA-15 MMM

1) PSf is dried in drying oven at 60-80 ºC for 12 hours to remove moisture.
2) The weightage of PSf, NMP and pristine SBA-15 are shown in Table 5 below. (Calculations are shown in appendix).

PSf (wt %)	SBA-15 (wt %)	NMP (wt %)
25.0	1.0	74.0
25.0	3.0	72.0
25.0	5.0	70.0

3) Pristine SBA-15 powder is slowly added into NMP while stirring.
4) PSf pallets are then added after SBA-15 dissolved.
5) Mixture is continuously left to stir for 12 hours.
6) Dope solution is then transferred to a centrifugal tube and sealed with parafilm for degassing purpose.
7) Degassing is carried out for 4 hours to remove the gas bubbles in dope solution.
8) After degassing is done, dope solution is left for standing in the lab at room temperature for 24 hours.
9) Dope solution is again put for degassing for 30 minutes and leave for standing 30 minutes to fully remove additional gas bubbles if necessary.
10) A clean glass plate is washed with acetone and dried completely using compressed air.
11) Dope solution is now ready to be casted. The homogenous mixture is poured onto the glass plate.
12) Membrane casting is then performed with the casting knife and film thickness is 200 µm.
13) The casting knife is pulled from upper to lower of the glass plate to form the membrane film. Speed should be consistent to prevent defects.
14) After casting, film is left to evaporate for 10 minutes on the glass plate.
15) Then, glass pate is immersed into coagulation bath which is half filled up with distilled water for 24 hours.
16) Membrane is finally dried in oven at 60 ºC for another 24 hours.

3.5 Experimental procedure: Fabrication of PSf/APTES/SBA-15 MMM

1) PSf is dried in drying oven at 60-80 ºC for 12 hours to remove moisture.
2) The weightage of PSf, NMP and APTES-modified SBA-15 are shown in Table 5 below. (Calculations are shown in appendix).

PSf (wt %)	APTES-modified SBA-15 (wt %)	NMP (wt %)
25.0	1.0	74.0
25.0	3.0	72.0
25.0	5.0	70.0

3) APTES-modified SBA-15 powder is slowly added into NMP while stirring.
4) PSf pallets are then added after SBA-15 dissolved.
5) Mixture is continuously left to stir for 12 hours.
6) Dope solution is then transferred to a centrifugal tube and sealed with parafilm for degassing purpose.
7) Degassing is carried out for 4 hours to remove the gas bubbles in dope solution.
8) After degassing is done, dope solution is left for standing in the lab at room temperature for 24 hours.
9) Dope solution is again put for degassing for 30 minutes and leave for standing 30 minutes to fully remove additional gas bubbles if necessary.
10) A clean glass plate is washed with acetone and dried completely using compressed air.
11) Dope solution is now ready to be casted. The homogenous mixture is poured onto the glass plate.
12) Membrane casting is then performed with the casting knife and film thickness is 200 µm.
13) The casting knife is pulled from upper to lower of the glass plate to form the membrane film. Speed should be consistent to prevent defects.
14) After casting, film is left to evaporate for 10 minutes on the glass plate.
15) Then, glass pate is immersed into coagulation bath which is half filled up with distilled water for 24 hours.
16) Membrane is finally dried in oven at 60 ºC for another 24 hours.

3.6 Project Activities

3.6.1 Synthesis of Pristine SBA-15

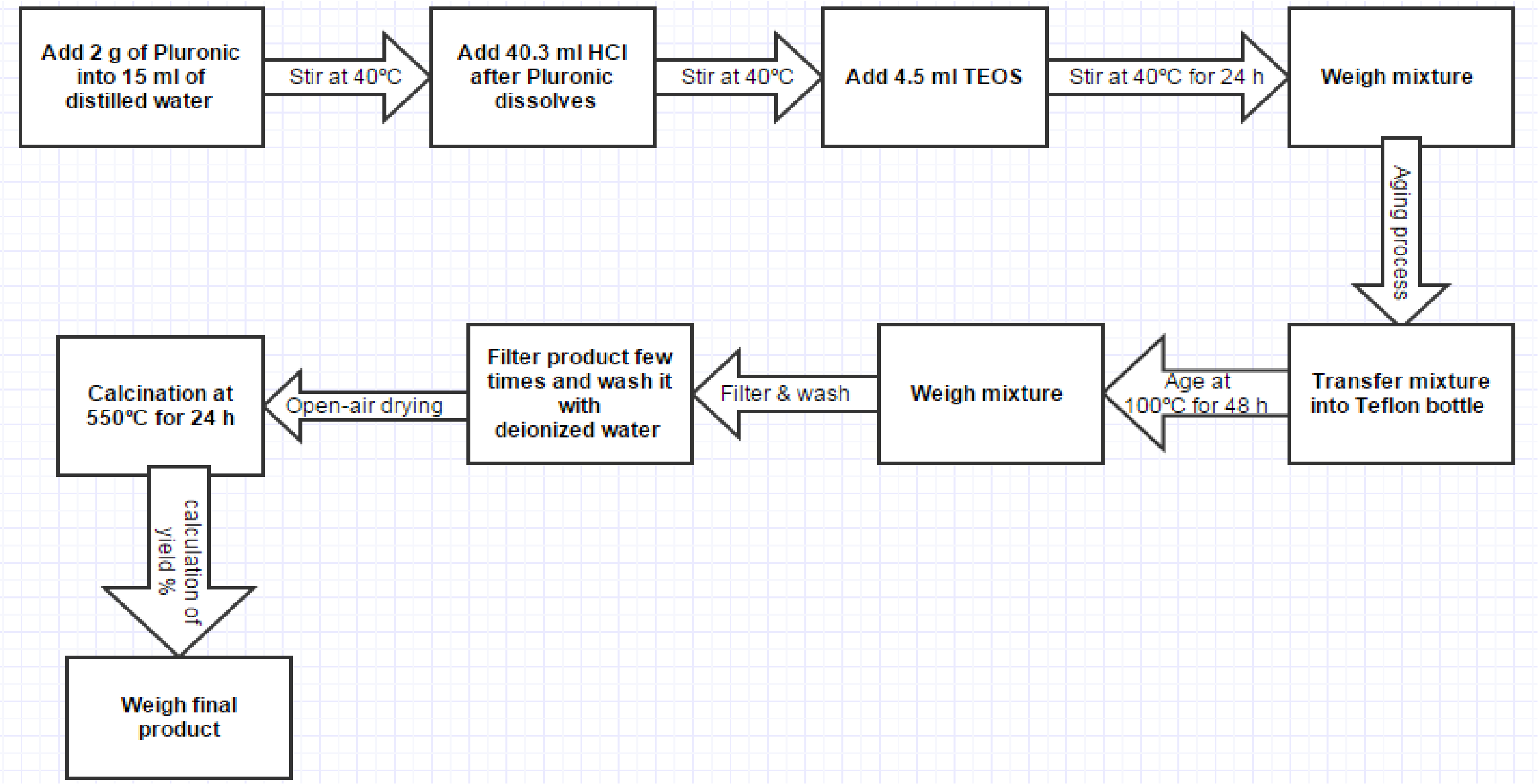

3.6.2 Synthesis of Functionalized SBA-15

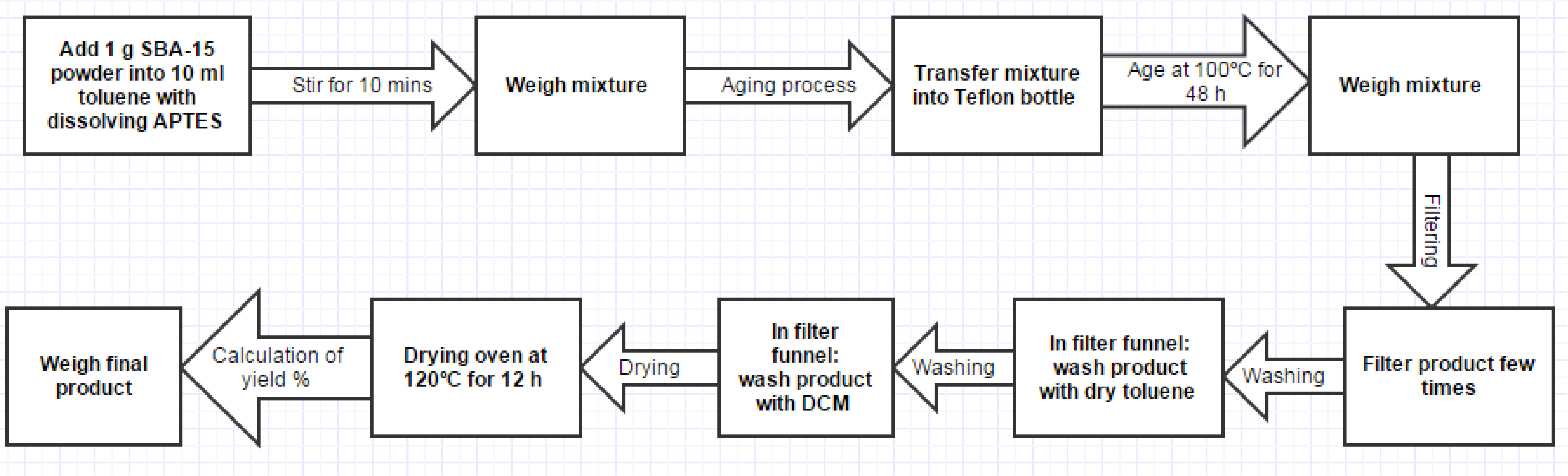

3.6.3 Synthesis of PSf Membrane and MMM

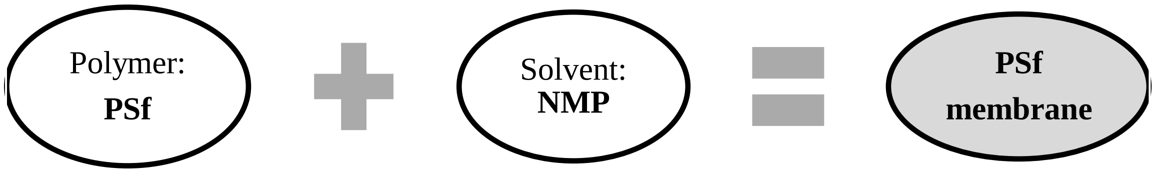

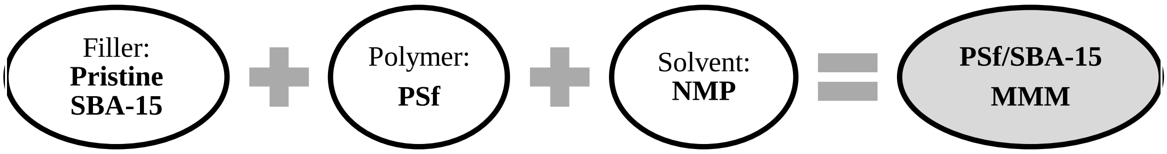

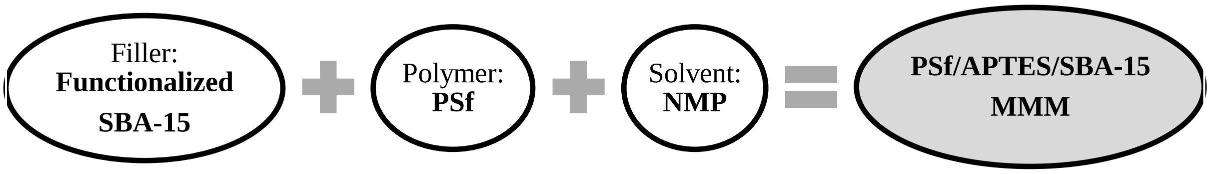

3.7 Characterization Techniques and Equipment

Table 3.1: Analytical tools used for characterization and its functions

Equipment	Purpose / Outcome
Field-Emission Scanning Electron Microscope /Energy Dispersive X-ray Analysis (FESEM/EDX Analysis) *Model: VP FESEM, Zeiss Supra 55*	To observe and analyze the surface area and cross-section morphology of membrane samples. Preparation before test: • Coat object with thin layer of conductor for current conduction. • Wash and dry material to below critical point to avoid damage of the fine structure. • Accelerating voltage: 3.0 kV • Runs sample at high pressure (20-40Pa) • Short working distance (2 to 5 mm)
Surface Area Analyzer and Porosimetry System (SAP) *Model: Micromeritics ASAP 2020*	• To observe the surface area structure and porosity of the sample. • The data were analyzed using the Broekoff-de Boer (BdB) model. Both adsorption and desorption branches were used to calculate the pore size distribution. • Pore volume and pore area distributions in the mesopore and macropore ranges by the BJH (Barrett, Joyner, and Halenda) method using a variety of thickness equations including a user defined, standard isotherm. • Sample tube is dried with nitrogen. • The surface area was calculated using the BET method.

Thermal Gravimetric Analyzer (TGA)	To determine the decomposition temperature and weight loss of the sample. Temperature Program: Heat from 100 °C to 900 °C @ 10 °C/minute in N_2 atmosphere with a purge rate of 20 mL/minute.
FTIR spectrometer	To determine the functional group in the sample according to the wavelengths from the spectra. Sample is crushed and compressed into a disc-liked structure for analysis.
Transmission Electron Microscope (TEM)	To observe and analyze the surface area of inorganic fillers for MMM. Sample is sonicated for one hour before analysis. Magnified images of SBA-15 obtained can be compared with previous studies.

CHAPTER 4

RESULTS AND DISCUSSION

4.1 Characterization Results of Pristine and Functionalized SBA-15

4.1.1 TEM images

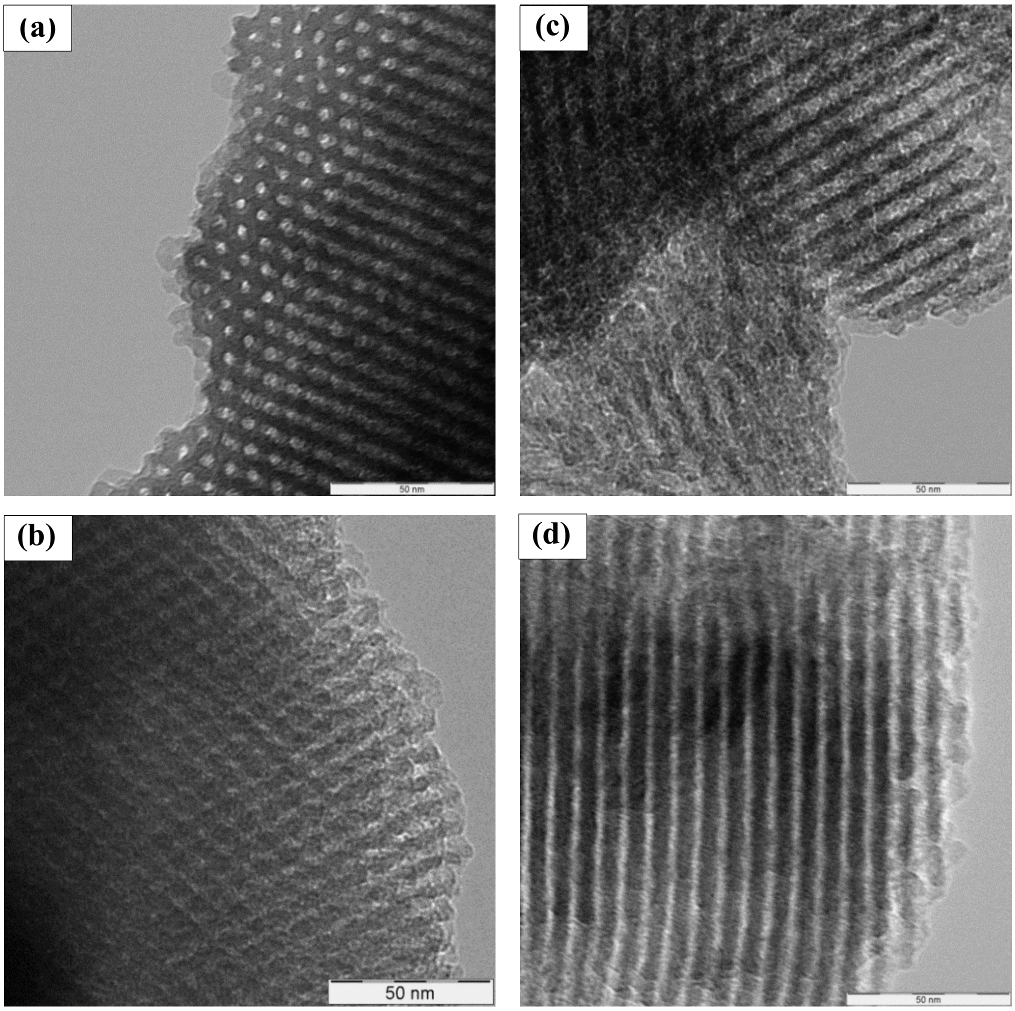

Figure 4.1: TEM images of (a) pristine SBA-15 in the direction of the pore axis, (b) functionalized SBA-15 in the direction of pore axis, (c) pristine SBA-15 in the direction perpendicular of the pore axis and (d) functionalized SBA-15 in the direction perpendicular of the pore axis.

The TEM images from pristine SBA-15 silica powder show a hexagonal array of uniform channels of averagely 4.5 nm in diameter. From the direction of the pore axis, it can be observed that SBA-15 has hexagonal structure, while from the perpendicular view it is seen as cylindrical pore channels. The hexagonal arrangement of mesostructured SBA-15 are in good agreement with Luan et al. (2005), Maria Chong and Zhao (2003) and Martín et al. (2015).

The TEM images of functionalized SBA-15 do not show significant difference in the spacing between channels form the one of the pristine SBA-15 mesoporous silica. This finding is supported by similar evidences from Luan et al. (2005). However, as mentioned by Martín et al. (2015) in his paper, functionalized silica particles generally show slight decrease in its textural properties compared to the pristine one, which is caused by the pore filling due to functionalization. Despite the change, functionalized SBA-15 still displays acceptable textural properties.

4.1.2 FTIR Spectra

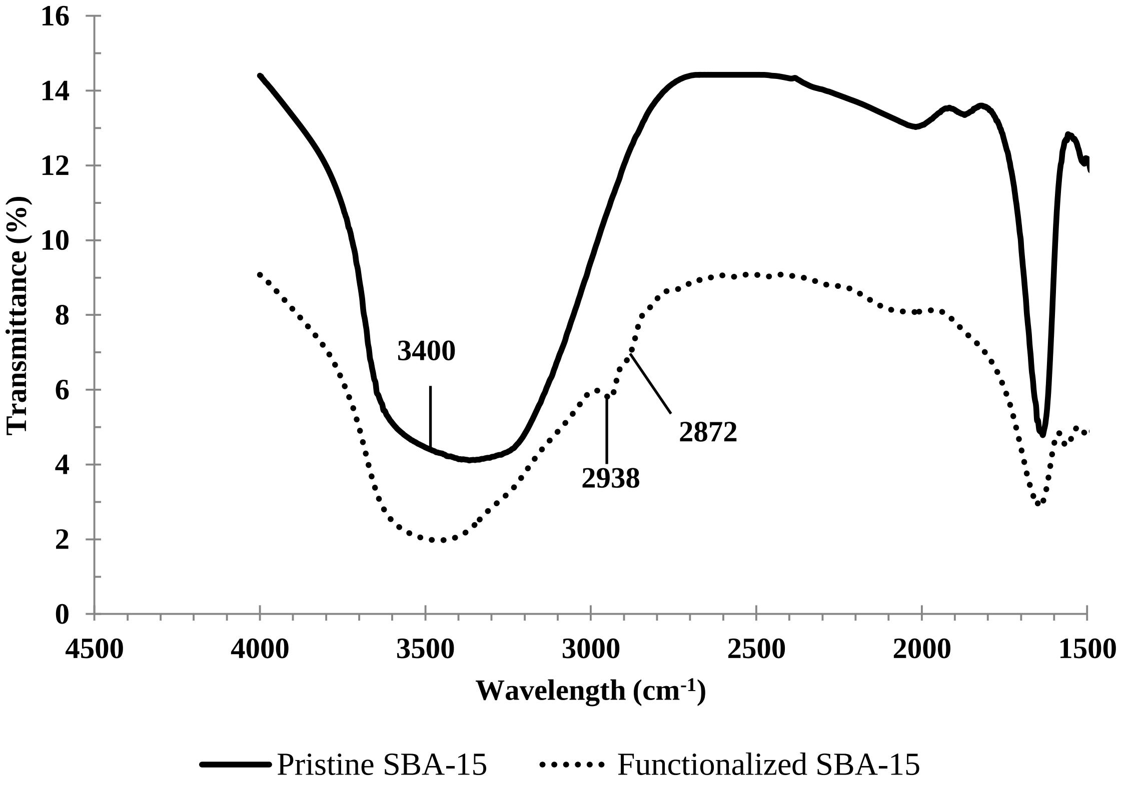

Figure 4.2: FTIR Spectra of pristine and functionalized SBA-15

Referring to Figure 4.2, the FTIR spectra of pristine and functionalized SBA-15 silica gives a low-frequency band centered at 3400cm^{-1} which is due to those silanol groups with cross hydrogen-bonding interactions in between. The presence of aminopropyl groups is identified by the appearance of C-H stretching bands at 2938cm^{-1} and 2872cm^{-1}. With this finding, it is proven that the aminopropyl groups are chemically bonded to the internal surface of SBA-15 silica; or in other words SBA-15 silica is successfully functionalized.

4.1.3 SAP Analysis

Table 4.1: SAP analysis of pristine SBA-15

BET surface area	727.19 m^2/g
Pore volume	1.22 cm^3/g
Pore size	66.93 Å

Table 4.2: SAP analysis of functionalized SBA-15

BET surface area	508.57 m^2/g
Pore volume	0.78 cm^3/g
Pore size	61.49 Å

Table 4.1 and 4.2 show SAP analysis of pristine and functionalized SBA-15. Pristine SBA-15 sample gives BET surface area of 727.19 m^2/g, pore volume of 1.22 cm^3/g and pore size of 66.93 Å. Meanwhile, functionalized SBA-15 has BET surface area of 508.57 m^2/g, pore volume of 0.78 cm^3/g and pore size of 61.49 Å. From the comparison of these two tables, functionalized SBA-15 has comparably lower values of three characteristics than that of pristine SBA-15.

This finding is contrasting to the expected result as functionalized SBA-15 is expected to show greater values in terms of surface area, pore volume and size. Although FTIR result shows APTES has been successfully incorporated into SBA-15, this SAP analysis shows that the functionalization step does not improve in terms of particles' surface areas, pore volumes and pore sizes.

4.2 Characterization Results of PSf Membrane and MMMs

4.2.3 FESEM Images

A preliminary study of 15wt%, 20wt%, 25wt% and 30wt% of PSf ratio to NMP experimental work was carried out to determine the optimum weight percent of PSf to be used in fabricating MMM. It is discovered that 25wt% of PSf is the best dope solution formulation for MMM as it has the most critical viscosity among all trials.

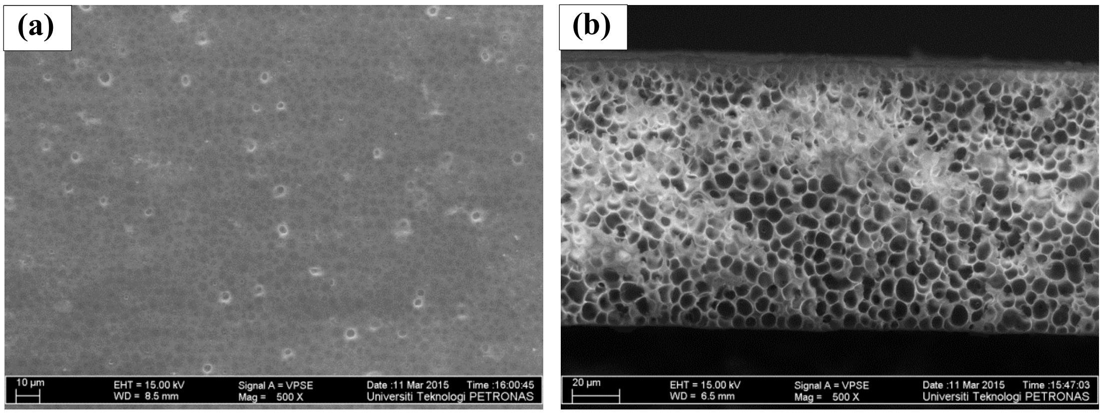

Figure 4.3: FESEM images of the surface (a) and cross -section (b) of the 25wt% PSf membrane.

The above analyzed PSf membrane has a thickness of 112.1 µm. During membrane casting, casting knife with thickness of 200 µm is used. From its cross-section image, the pores of the membrane can be seen. PSf membrane is commonly used currently in the industry for gas separation application. CO_2 will be trapped inside the pores of the membrane to remove it from natural gas.

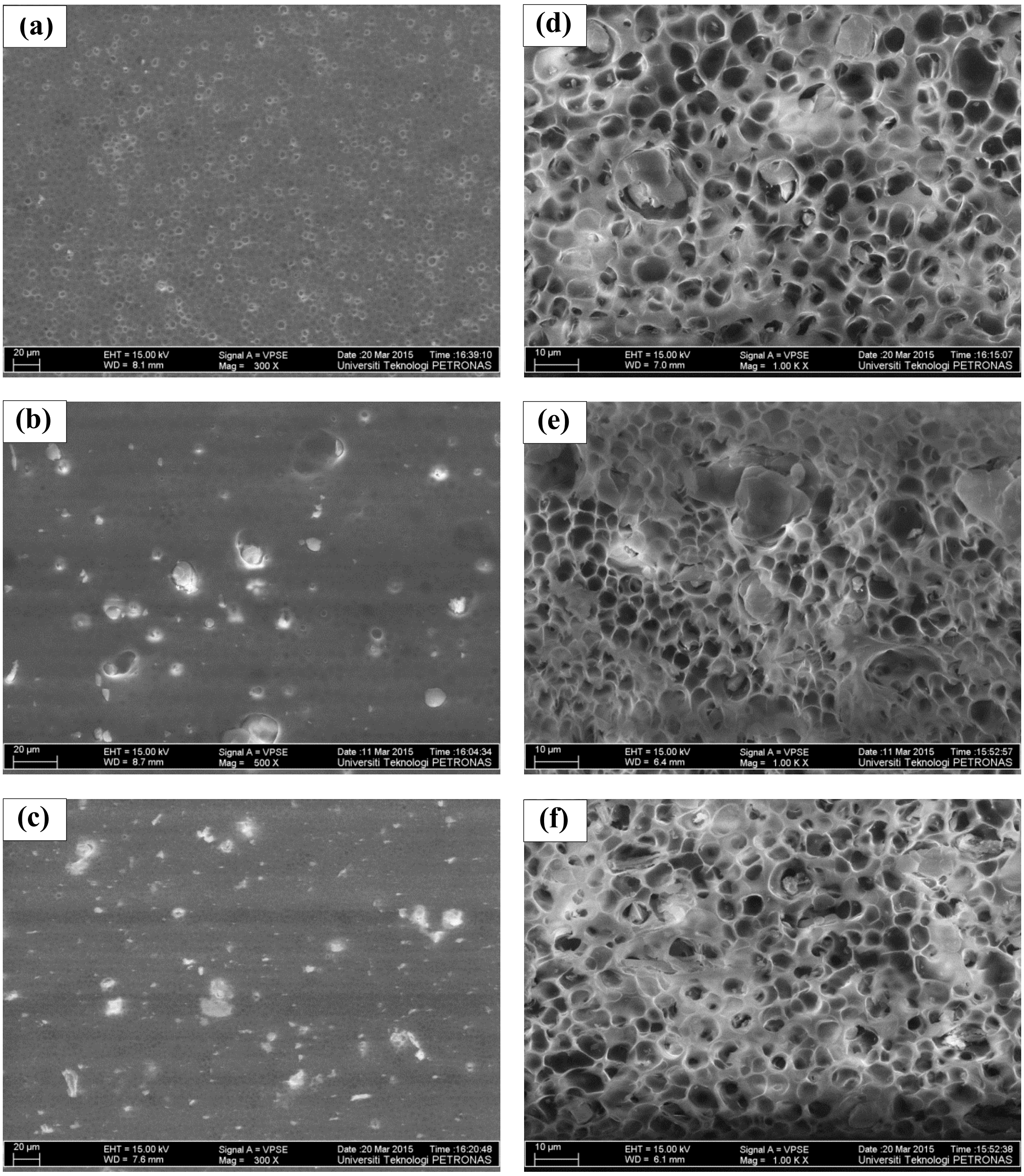

Figure 4.4: FESEM images of the surface of different SBA-15 loadings (a) 1wt%, (b) 3wt% and (c) 5wt%; and cross-section images of (d) 1wt%, (e) 3wt% and (f) 5wt% of PSf/pristine SBA-15 MMM.

The morphology of MMMs strongly affects its gas separation performance. Hence, FESEM is utilized to study the extent of the adhesion between filler particles and polymer matrix. The MMMs surface area and cross-sectional morphologies are shown in Figure 4.4. From Figure 4.4(a), it is observed that the presence of pristine SBA-15 can hardly be detected from its surface area because of the low fillers concentration. Above images of MMMs show good distribution but moderate dispersion of SBA-15 fillers. From Figure 4.4(b), particles agglomeration is identified. There is however minimal formation of voids surrounding the SBA-15 particles. This proves that there is good adhesion between the filler particles and the PSf polymer matrix. This is speculated to be the result of a high degree of compatibility between the filler particles and the polymer matrix.

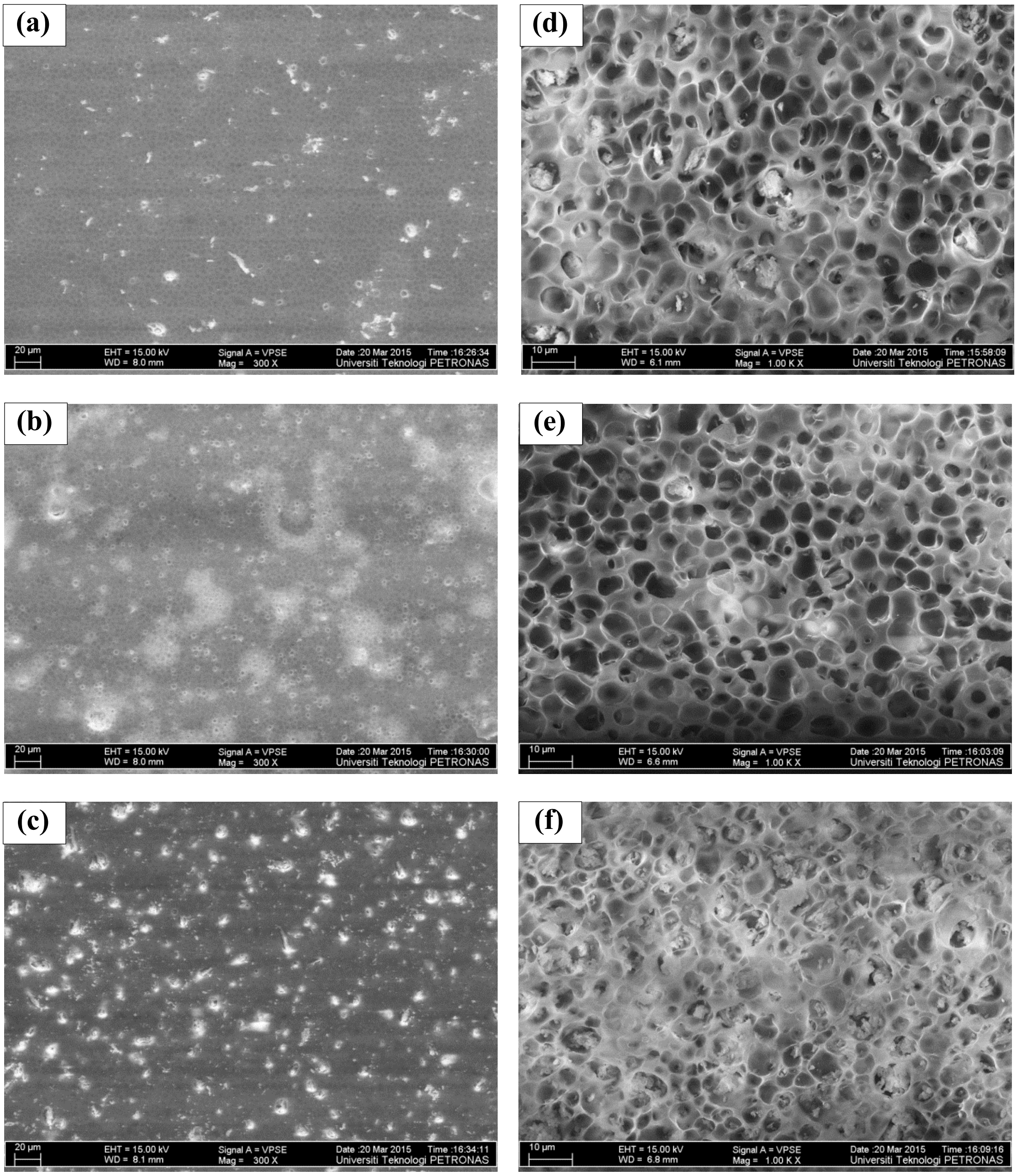

Figure 4.5: FESEM images of the surface of different SBA-15 loadings (a) 1wt%, (b) 3wt% and (c) 5wt%; and cross-section images of (d) 1wt%, (e) 3wt% and (f) 5wt% of PSf/functionalized SBA-15 MMM.

Figure 4.5 illustrates the effect of different loadings of SBA-15 fillers on the MMMs morphology. As can be seen, by increasing the filler loading, the contact among the particles was increased, hence particle agglomeration is observed. This shows a deviation from the expected ideal morphology. Figure 4.5(c) shows obvious agglomeration of the filler particles with loading of 5wt%. Hashemifard and Ismail (2011) also mention in their journal that the increase in extend of particles agglomeration resulted in void formation, which will lead to a decrease in the MMMs separation performance.

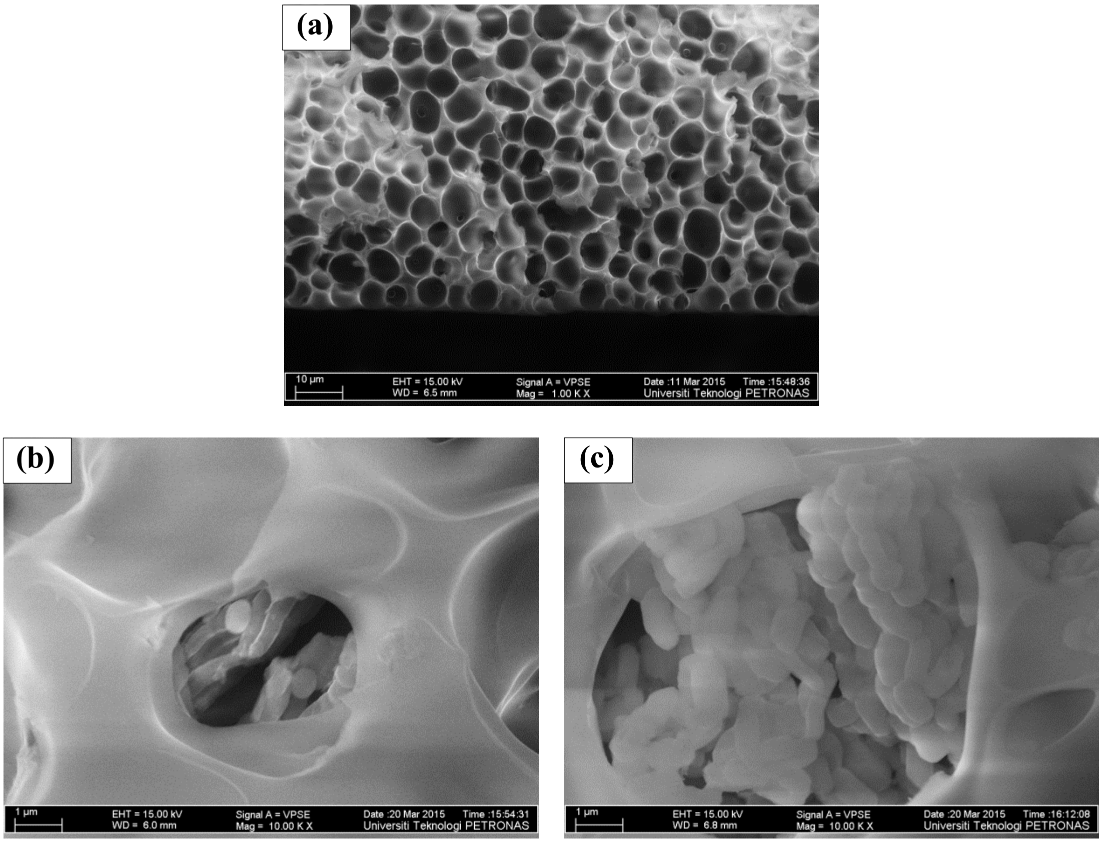

Figure 4.6: Close-up of membranes pores: (a) PSf membrane, (b) PSf/pristine SBA-15 MMM and (c) PSf/functionalized SBA-15 MMM.

From Figure 4.6, functionalized SBA-15 incorporated into MMMs also shows similarly good distributions throughout the surface area as compared to that of the pristine one. As the loadings of SBA-15 fillers increase, filler particles are distributed more evenly at the membrane surface. Figure 4.6 shows the interfacial adhesion of pristine and functionalized SBA-15 MMMs. PSf/pristine SBA-15 MMM has interfacial voids formed at the PSf-SBA-15 interface, while PSf/functionalized SBA-15 MMM has better adhesion with minimal voids formed.

Voids formation at the interface is known as ‘sieve-in-a-cage’ morphology, which has considerable effect on membranes performance. Voids provide the path of the least resistance, so gas molecules pass through them instead of sieve particles, causing much higher permeability as compared to that of the PSf membrane. The functionalization of SBA-15 fillers is used as adhesion promoters between the sieve and the polymer. Maria Chong and Zhao (2003) concluded that the functionalization of mesoporous SBA-15 by co-condensation of tetraethoxysilane (TEOS) with organosilane (aminopropyl) triethoxysilane (APTES) enables a better control of the pore size and the density of functional groups. Hence, the incorporation of SBA-15 fillers to MMMs is believed to be able to improve its permeability and selectivity in comparison with the PSf membrane.

4.2.4 EDX Analysis

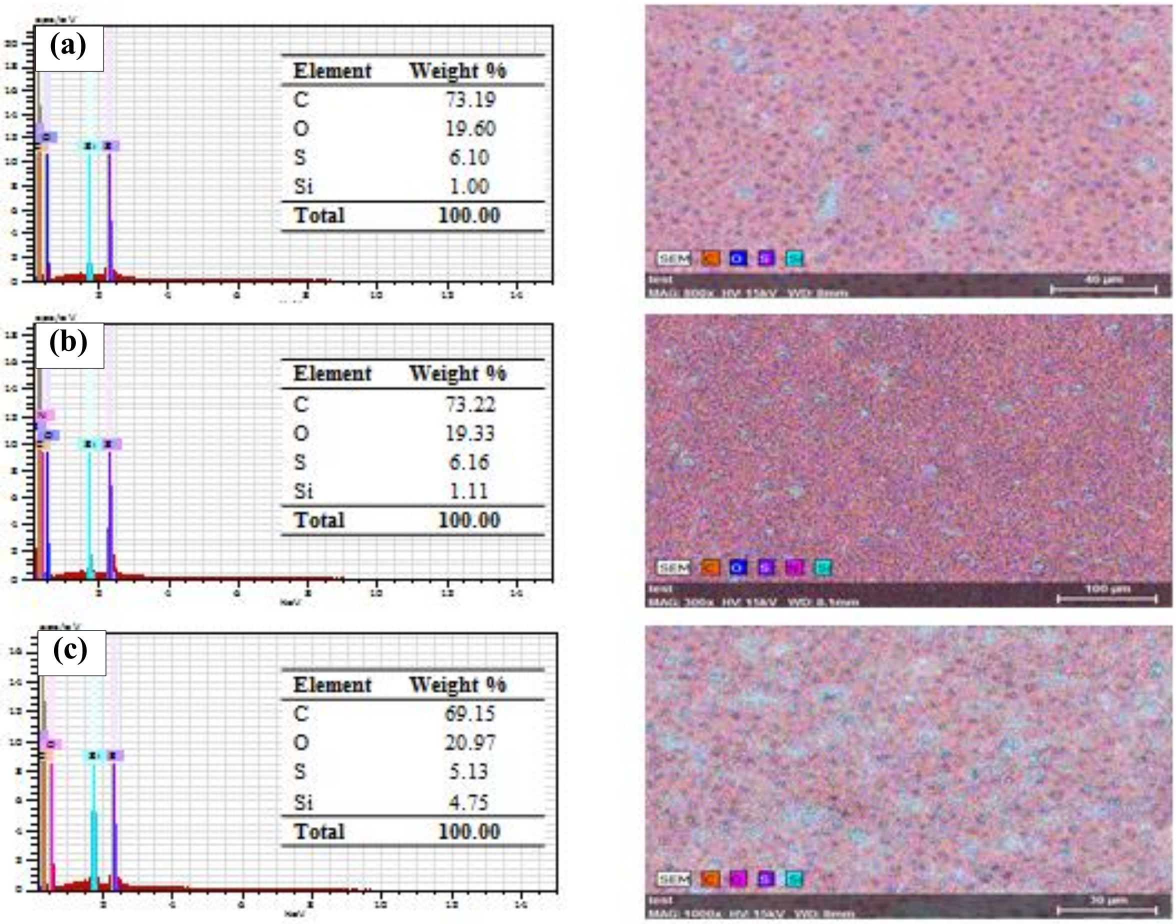

(a)

Element	Weight %
C	73.19
O	19.60
S	6.10
Si	1.00
Total	**100.00**

(b)

Element	Weight %
C	73.22
O	19.33
S	6.16
Si	1.11
Total	**100.00**

(c)

Element	Weight %
C	69.15
O	20.97
S	5.13
Si	4.75
Total	**100.00**

Figure 4.7: EDX graphs and mapping of PSf/SBA-15 MMM with different SBA-15 loadings of (a) 1wt%, (b) 3wt% and (c) 5wt%.

From Figure 4.7, EDX graphs show the weight percentage of elements in MMMs. The element of Si confirms the incorporation of SBA-15 while the element of S shows the presence of PSf polymer matrix in MMMs. The weight percentage of Si element increases when the SBA-15 loading increases. EDX mapping on the right side shows the distribution of SBA-15 in the membrane structure. As the SBA-15 loading increases, the distribution gets better as it is well-distributed throughout the surface area of the membranes. However, particle agglomerations are detected as well.

4.2.5 TGA Curves

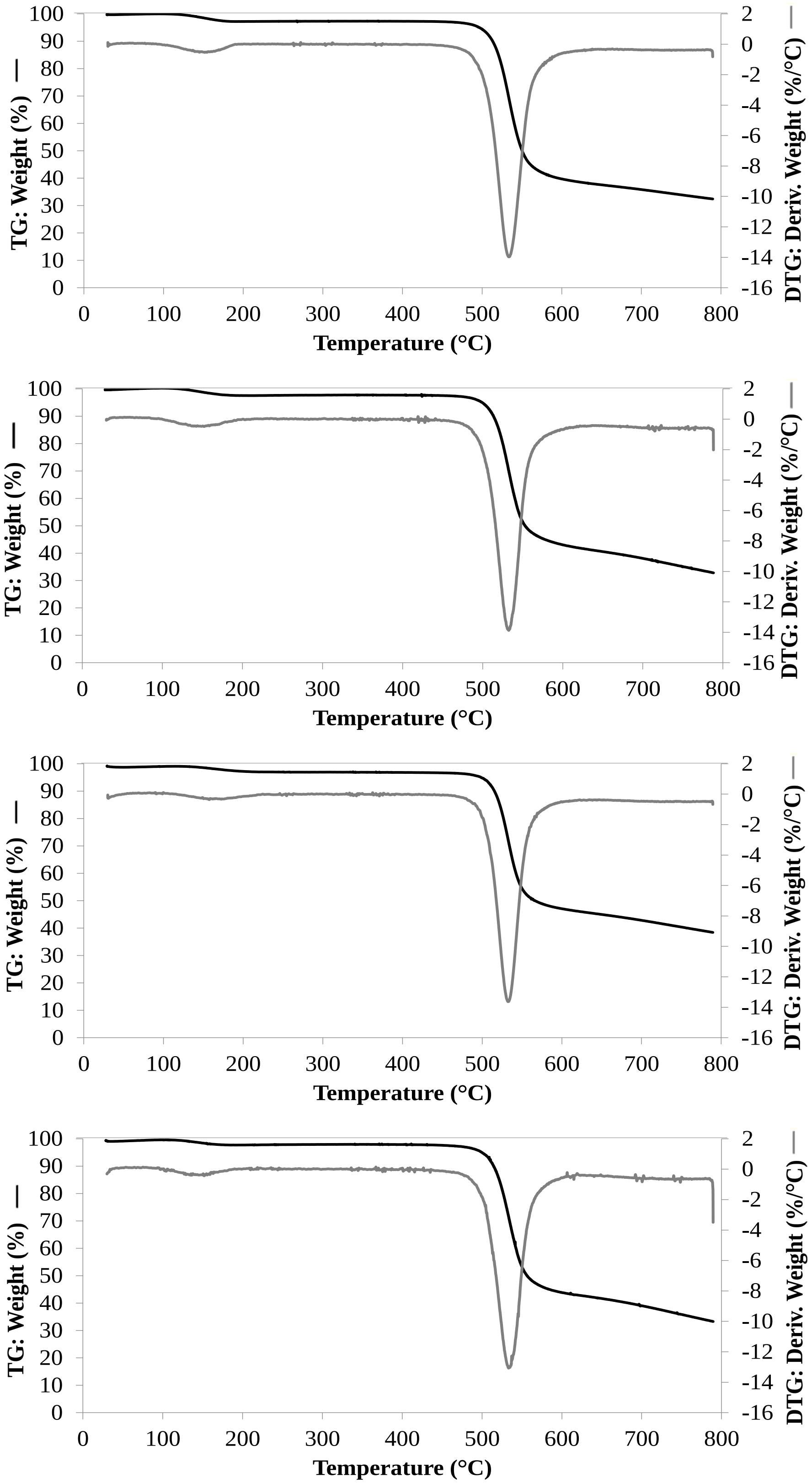

Figure 4.8: TG and DTG curves of membranes: (a) PSf membrane, (b) PSf/1wt% pristine SBA-15 MMM, (c) PSf/3wt% pristine SBA-15 MMM and (d) PSf/3wt% functionalized SBA-15 MMM.

Figure 4.8 illustrates the weight loss curves of PSf membrane and MMMs. In the curve of the PSf membrane and PSf/1wt% pristine SBA-15 MMM, one minor weight loss is resolved at 150°C, which corresponding to the weight loss of the NMP solvent in the membranes. A major weight loss in the range of the analysis corresponds to the DTG peak at 535°C. For the MMMs with 3wt% and 5wt% loadings, the same major weight loss stages are shown in Figure 13(c) and (d). According to the DTG curves, the peak is 530°C for 3wt% SBA-15 MMM and 540°C for 5wt% SBA-15 MMM. From Figure 4.8, it is observed that the thermal profiles of these four membranes are generally similar.

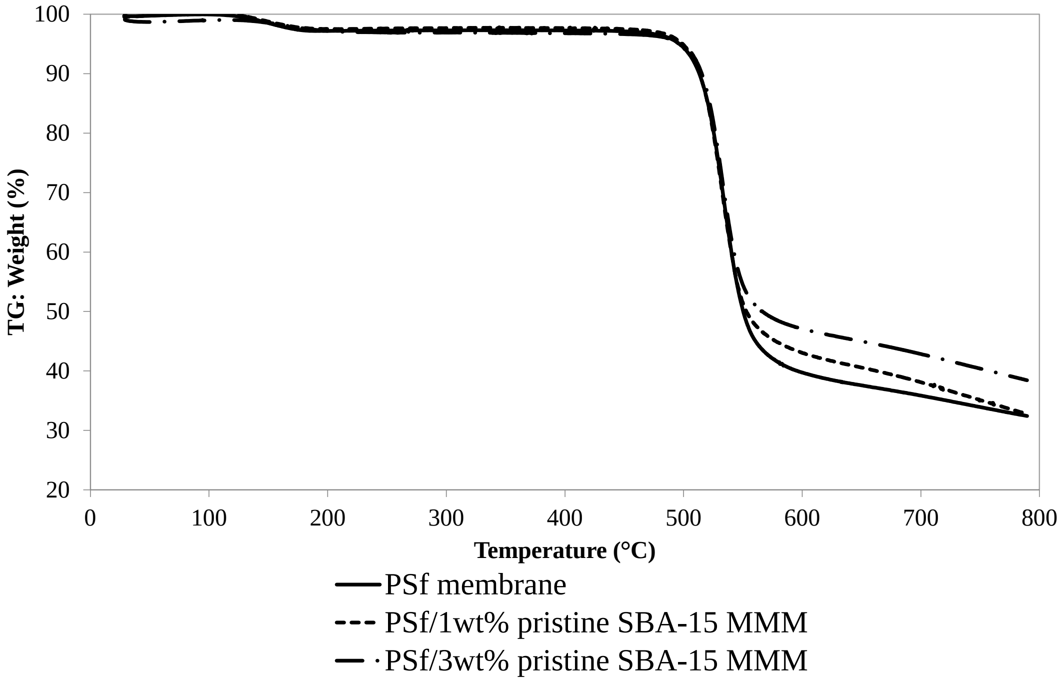

Figure 4.9: Comparison of TG curves: PSf membrane and PSf/pristine SBA-15 MMMs

Figure 4.9 shows the TG curves or PSf membrane and MMMs, where the final residue loss of MMMs is higher than that of PSf membrane. This shows that the incorporation of SBA-15 fillers to form MMM has better gas separation performance than PSf membrane. This phenomenon is in good agreement with the above FESEM interpretation.

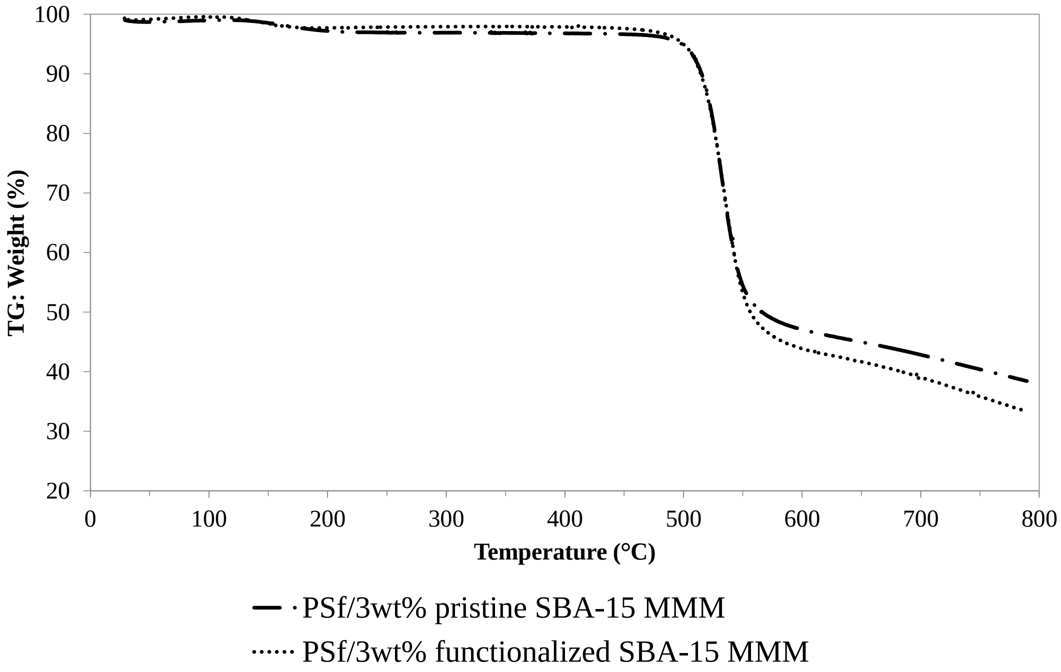

Figure 4.10: Comparison of TG curves: PSf/pristine SBA-15 MMM and PSf/functionalized SBA-15 MMM

In Figure 4.10, when the comparison between pristine and functionalized SBA-15 in MMM is done, it is found that the final residue loss of pristine SBA-15 fillers MMM is higher than the functionalized one. This is contradicting to the expected result, but matches the SAP analysis discussed above. It is again to be concluded here that functionalized SBA-15 does not proved to produce better result than pristine SBA-15 fillers when incorporated into PSf polymer matrix.

CHAPTER 5

CONCLUSION AND RECOMMENDATIONS

5.1 Conclusion

A batch of approximately 1.1g of pristine SBA-15 mesoporous silica powder is successfully synthesized within 5 days of experimental work. Functionalization of SBA-15 is then carried out by incorporating APTES into the SBA-15 powder. Pristine and functionalized SBA-15 is then characterized by using analytical tools TEM, FTIR and SAP. From the TEM images functionalized SBA-15 shares similar morphology as the pristine one, which is hexagonal pore structure with cylindrical pore channels. APTES is proven to be successfully incorporated into SBA-15 surface with the presence of C-H bands in its FTIR spectrum.

PSf/SBA-15 MMMs are fabricated with different pristine and functionalized SBA-15 loadings to investigate on its morphology and cross-section structures. As the SBA-15 loadings increases, particles agglomeration increases as well. MMMs with 1wt% SBA-15 is hardly to be detected from its surface and cross-section. Hence, SBA-15 with 3wt% loadings is concluded to be the optimum percentage incorporated into MMM to enhance its gas separation performance. TGA results show that the average weight decomposition temperature of all membranes is about 530°C. Functionalized SBA-15 MMM shows better thermal properties than the pristine SBA-15 MMM.

From FESEM analysis, SBA-15 fillers are seen to be well-distributed throughout the surface of the MMMs with moderate dispersion as particles agglomeration was identified. Functionalized SBA-15 shows better interfacial adhesion with lesser voids formation. Hence, MMMs with incorporation of either pristine or functionalized SBA-15 fillers are expected to enhance its separation performance as compared to that of the PSf membrane.

5.2 Recommendations

Upon completing this project, there are few recommendations to be highlighted to improve on the project result. These recommendations can be implemented if this project were to be extended. Some of the recommendations are:

- To synthesize nano-scaled SBA-15 silica powder

Nano particles inorganic fillers are believed to be able to improve gas separation better. In this project, the goal of synthesizing SBA-15 in nano-scaled was not achieved as the time frame for project completion is short.

- To solve particle agglomerations problem

From the FESEM images, particles agglomeration was identified and this defect will affect the CO_2/CH_4 separation. This problem should be analyzed to identify the contributing factors, which can be from the experimental procedure steps. To prevent the aggregation of the particles and improve adhesion at the surface, especially at higher loadings, a priming protocol is suggested. The SBA-15 fillers can be dispersed into NMP and a small amount of PSf polymer, and mixed it overnight.

- To functionalize SBA-15 with other potential functional groups

After this project is completed, aminopropyl group might not be the best functional group to be incorporated with SBA-15 fillers as the result has deviated from the expected one. Research has been done that SBA-15 can be functionalized with silanol groups as well in improving its performance. Preliminary studies should be done to understand better the functionalization procedures of each functional group.

- To perform gas permeation experiment for resultant MMMs

Due to time constraint and large scope to be covered, resultant membrane and MMMs were not tested for its gas separation performance by using the gas permeation rig. The permeability and selectivity of the fabricated membranes can be studied and analyzed if this project is being continued.

REFERENCES

Beck, JS, Vartuli, JC, Roth, WJ, Leonowicz, ME, Kresge, CT, Schmitt, KD, Sheppard, EW. (1992). A new family of mesoporous molecular sieves prepared with liquid crystal templates. *Journal of the American Chemical Society, 114*(27), 10834-10843.

Brunetti, A, Scura, F, Barbieri, G, & Drioli, E. (2010). Membrane technologies for CO_2 separation. *Journal of Membrane Science, 359*(1), 115-125.

Cao, Liang, Man, Tiffany, & Kruk, Michal. (2009). Synthesis of ultra-large-pore SBA-15 silica with two-dimensional hexagonal structure using triisopropylbenzene as micelle expander. *Chemistry of Materials, 21*(6), 1144-1153.

Chung, Tai-Shung, Jiang, Lan Ying, Li, Yi, & Kulprathipanja, Santi. (2007). Mixed matrix membranes (MMMs) comprising organic polymers with dispersed inorganic fillers for gas separation. *Progress in Polymer Science, 32*(4), 483-507.

Eren, Erdal, Sarihan, Adem, Eren, Bilge, Gumus, Huseyin, & Kocak, Fadime Ozdemir. (2015). Preparation, characterization and performance enhancement of polysulfone ultrafiltration membrane using PBI as hydrophilic modifier. *Journal of Membrane Science, 475*, 1-8. doi: 10.1016/j.memsci.2014.10.010

Freeman, Benny D. (1999). Basis of permeability/selectivity tradeoff relations in polymeric gas separation membranes. *Macromolecules, 32*(2), 375-380.

Hashemifard, SA, & Ismail, Ahmad Fauzi. (2011). Effects of montmorillonite nano-clay fillers on PEI mixed matrix membrane for CO_2 removal. *Chemical Engineering Journal, 170*(1), 316-325.

He, Li, Li, Dan, Wang, Kun, Suresh, Akkihebbal K, Bellare, Jayesh, Sridhar, Tam, & Wang, Huanting. (2011). Synthesis of silicalite-poly (furfuryl alcohol) composite membranes for oxygen enrichment from air. *Nanoscale research letters, 6*(1), 1-9.

Hu, Q, Marand, E, Dhingra, S, Fritsch, D, Wen, J, & Wilkes, G. (1997). Poly (amide-imide) TiO_2 nano-composite gas separation membranes: Fabrication and characterization. *Journal of membrane Science, 135*(1), 65-79.

Huang, Yulin. (2009). Functionalization of mesoporous silica nanoparticles and their applications in organo-, metallic and organometallic catalysis.

Iglesias, Jose, Melero, Juan A., & Sainz-Pardo, Javier. (2008). Direct synthesis of organically modified Ti-SBA-15 materials. *Journal of Molecular Catalysis A: Chemical, 291*(1-2), 75-84. doi: 10.1016/j.molcata.2008.06.004

Ismail, AF, & Lorna, W. (2002). Penetrant-induced plasticization phenomenon in glassy polymers for gas separation membrane. *Separation and purification technology, 27*(3), 173-194.

Ismail, Ahmad Fauzi, & Mansourizadeh, A. (2010). A comparative study on the structure and performance of porous polyvinylidene fluoride and polysulfone hollow fiber membranes for CO_2 absorption. *Journal of Membrane Science, 365*(1), 319-328.

Johansson, Emma M. (2010). Controlling the Pore Size and Morphology of Mesoporous Silica.

Julian, Helen, & Wenten, IG. (2012). Polysulfone membranes for CO_2/CH_4 separation: state of the art. *J. Eng, 2*(3), 484-495.

Kruk, Michal, Jaroniec, Mietek, Ko, Chang Hyun, & Ryoo, Ryong. (2000). Characterization of the porous structure of SBA-15. *Chemistry of materials, 12*(7), 1961-1968.

Li, Norman N, Fane, Anthony G, Ho, WS Winston, & Matsuura, Takeshi. (2011). *Advanced membrane technology and applications*: John Wiley & Sons.

Luan, Zhaohua, Fournier, Jay A., Wooten, Jan B., & Miser, Donald E. (2005). Preparation and characterization of (3-aminopropyl) triethoxysilane-modified mesoporous SBA-15 silica molecular sieves. *Microporous and Mesoporous Materials, 83*(1-3), 150-158. doi: 10.1016/j.micromeso.2005.04.006

Margolese, D, Melero, JA, Christiansen, SC, Chmelka, BF, & Stucky, GD. (2000). Direct syntheses of ordered SBA-15 mesoporous silica containing sulfonic acid groups. *Chemistry of Materials, 12*(8), 2448-2459.

Maria Chong, AS, & Zhao, XS. (2003). Functionalization of SBA-15 with APTES and characterization of functionalized materials. *The Journal of Physical Chemistry B, 107*(46), 12650-12657.

Martín, Antonio, Arsuaga, Jesús M, Roldán, Nuria, de Abajo, Javier, Martínez, Ana, & Sotto, Arcadio. (2015). Enhanced ultrafiltration PES membranes doped with mesostructured functionalized silica particles. *Desalination, 357*, 16-25.

Moghadassi, A. R., Rajabi, Z., Hosseini, S. M., & Mohammadi, M. (2014). Fabrication and modification of cellulose acetate based mixed matrix membrane: Gas separation and physical properties. *Journal of Industrial and Engineering Chemistry, 20*(3), 1050-1060. doi: 10.1016/j.jiec.2013.06.042

Morooka, Shigeharu, & Kusakabe, Katsuki. (1999). Microporous Inorganic Membranes for Gas Separation. *MRS Bulletin, 24*(03), 25-29. doi: doi:10.1557/S0883769400051873

Rezakazemi, Mashallah, Ebadi Amooghin, Abtin, Montazer-Rahmati, Mohammad Mehdi, Ismail, Ahmad Fauzi, & Matsuura, Takeshi. (2014). State-of-the-art membrane based CO_2 separation using mixed matrix membranes (MMMs): An overview on current status and future directions. *Progress in Polymer Science, 39*(5), 817-861. doi: 10.1016/j.progpolymsci.2014.01.003

Sakpal, Tushar, Kumar, Asheesh, Kamble, Sanjay, & Kumar, Rajnish. (2012). Carbon dioxide capture using amine functionalized silica gel. *Indian Journal of Chemistry-Part A InorganicPhysical Theoretical and Analytical, 51*(9), 1214.

Srivastava, R., Srinivas, D., & Ratnasamy, P. (2005). CO_2 activation and synthesis of cyclic carbonates and alkyl/aryl carbamates over adenine-modified Ti-SBA-15 solid catalysts. *Journal of Catalysis, 233*(1), 1-15. doi: 10.1016/j.jcat.2005.03.023

Staiger, Chad L, Pas, Steven J, Hill, Anita J, & Cornelius, Chris J. (2008). Gas separation, free volume distribution, and physical aging of a highly microporous spirobisindane polymer. *Chemistry of Materials, 20*(8), 2606-2608.

Vivero-Escoto, Juan L, Slowing, Igor I, Trewyn, Brian G, & Lin, Victor S-Y. (2010). Mesoporous silica nanoparticles for intracellular controlled drug delivery. *Small, 6*(18), 1952-1967.

Yan, X., Komarneni, S., & Yan, Z. (2013). CO2 adsorption on Santa Barbara Amorphous-15 (SBA-15) and amine-modified Santa Barbara Amorphous-15 (SBA-15) with and without controlled microporosity. *J Colloid Interface Sci, 390*(1), 217-224. doi: 10.1016/j.jcis.2012.09.038

Zhang, Yuan, Sunarso, Jaka, Liu, Shaomin, & Wang, Rong. (2013). Current status and development of membranes for CO_2/CH_4 separation: A review. *International Journal of Greenhouse Gas Control, 12*, 84-107.

Zhao, Dongyuan, Huo, Qisheng, Feng, Jianglin, Chmelka, Bradley F, & Stucky, Galen D. (1998). Nonionic triblock and star diblock copolymer and oligomeric surfactant syntheses of highly ordered, hydrothermally stable, mesoporous silica structures. *Journal of the American Chemical Society, 120*(24), 6024-6036.

Zheng, Feng, Tran, Diana N, Busche, Brad J, Fryxell, Glen E, Addleman, R Shane, Zemanian, Thomas S, & Aardahl, Christopher L. (2005). Ethylenediamine-modified SBA-15 as regenerable CO_2 sorbent. *Industrial & engineering chemistry research, 44*(9), 3099-3105.

APPENDIX

Calculations

A. To obtain standard solution of 2 M of HCl

Current weight percent of HCl = 37.7 %

Density of HCl = 1.19 g/mL

Molecular weight of HCl = 36.46 g/mol

<u>Step 1: Determine moles of HCl in 100g of 37.7 % solution</u>

$$Moles\ of\ HCl\ =\ 37.7\ g\ of\ HCl\ \times\ \frac{1\ mol}{36.46\ g\ of\ HCl} = 1.03\ mol$$

<u>Step 2: Determine volume of 100 g of a solution</u>

$$Density = \frac{mass}{volume}$$

$$Volume = \frac{100\ g}{1.19\frac{g}{mL}} = 84.03\ mL = 0.08403\ L$$

<u>Step 3: Determine the molarity of 37.7wt% of HCl solution</u>

$$Molarity\ of\ HCl = \frac{1.03\ mol}{0.08403\ L} = 12.3\frac{mol}{L} = 12.3\ M$$

<u>Step 4: Determine the volume of HCl needed to obtain 1 L of 2 M HCl solution</u>

$$\frac{2\ M\ HCl\ (needed)}{12.3\ M\ HCl\ (current)} \times 1000\ ml = 162.6\ ml$$

∴ Approximately <u>162 ml</u> of 37.7 wt% HCl is needed to obtain a standard solution of 2 M HCl.

B. To calculate volume and weight adjusted when weight percent, wt% is given

To fabricate pristine PSf membrane, we need <u>25 wt% of PSf</u> and <u>75 wt% for NMP</u>; <u>dope solution is 10mL</u>:

Density $_{\text{PSf}}$ = 1.24 g/mL

Density $_{\text{NMP}}$ = 1.03 g/mL

Taking <u>100 gram as basis</u>,

Weight $_{\text{PSf}}$ = 25 g; weight $_{\text{NMP}}$ = 75 g

Volume $_{\text{PSf}}$ = $\frac{Weight_{PSf}}{Density_{PSf}} = \frac{25\ g}{1.24\ g/mL} = 20.16\ mL$

Volume $_{\text{NMP}}$ = $\frac{Weight_{NMP}}{Density_{NMP}} = \frac{75\ g}{1.03\ g/mL} = 72.82\ mL$

Volume $_{\text{PSf + NMP}}$ = 20.16 + 72.82 mL = 92.97 mL

Volume adjusted $_{\textbf{NMP}}$ = $Volume_{NMP} \times \frac{Volume_{\ dope\ solution}}{Volume_{\ PSf+NMP}}$

= $72.82\ mL \times \frac{10\ mL}{92.97\ mL}$

= **7.83 mL**

Volume adjusted $_{\text{PSf}}$ = $Volume_{PSf} \times \frac{Volume_{\ dope\ solution}}{Volume_{\ PSf+NMP}}$

= $20.16\ mL \times \frac{10\ mL}{92.97\ mL}$

= 2.17 mL

Weight adjusted $_{\textbf{PSf}}$ = $\frac{Volume\ adjusted_{PSf}}{Density_{PSf}}$

= $2.17\ mL \times 1.24\ g/mL$

= **2.69 g**